



# PERFORMANCE ANALYSIS OF DATA STRUCTURES FOR UNSTRUCTURED GRID SOLUTIONS ON FINITE VOLUME SIMULATIONS

## Fernanda Paula Barbosa

Instituto de Ciências Matemáticas e de Computação, USP - ICMC, São Carlos, SP, 13566-590, Brazil  
 ferpaula@icmc.usp.br

## Ives Renê Venturini Pola

Instituto de Ciências Matemáticas e de Computação, USP - ICMC, São Carlos, SP, 13566-590, Brazil  
 ives@icmc.usp.br

## Antonio Castelo Filho

Instituto de Ciências Matemáticas e de Computação, USP - ICMC, São Carlos, SP, 13566-590, Brazil  
 castelo@icmc.usp.br

**Abstract.** *The efficient storage and access of grids by data structures using topological operators is one of the most important goals of the geometric modeling research field. It usually requires less time to load grid files and allows efficient query operations. Topological data structures index elements of grid representing incidence and adjacency properties. One of most common aspects from problems solved by computational fluid mechanics is the complexity of the domain's geometry. The usage of data structures to index computational grids is of great importance because it performs queries efficiently and places all grid operations on a unique module, allowing its extension to aid diverse applications. This work aims at exploring the coupling of a topological data structure, the Mate Face, into a solver module, by controlling all grid access by providing operators and iterators that perform complex neighbor queries. The solver module solves the governing equations from fluid mechanics through the finite volume technique with a formulation that sets the property values to the control volume centroids, using high order methods - the ENO and WENO schemes. The two dimensional Euler equations are considered to represent the flows of interest. The coupling of the Mate Face data structure to the solver module was achieved by a creation of a library that acts as an interface layer between modules, the Mate Face and the solver, which had been implemented using different programming languages. Therefore, all Mate Face class methods are available to the solver module through the interface library in the form of procedures. Experiments measuring the computational cost of using the Mate Face data structure comparing with the traditional tables representation of grids show that the Mate Face is faster to build and presents less memory occupation rate when indexing grids with a higher number of elements. Moreover, experiments were performed to validate the usage of the Mate Face along with numeric methods. Finally, the data structure can aid the fluid flow simulation tools by managing the grid file and providing efficient query operators.*

**Keywords:** *Numerical Simulation, Topological Data Structure, WENO Schemes, Finite Volume Method.*

## 1. INTRODUCTION

Numerical simulations that with high Mach values produce strong discontinuities, i.e., shock waves occurring on the studied dynamic flows. Some approaches in literature were proposed, such as the upwind schemes, the flow vector separation Van Leer (1982) Liou (1996), and tested using the linear reconstruction scheme MUSCL Anderson (1963), generating discretizations with second order on the spatial precision. Besides that, there is an effective reduction in the precision order in such second order of nominal precision when we have non structured meshes Azevedo *et al.* (2010). Therefore, reconstructions of MUSCL type lead to schemes of the total variation reduction TVD, where schemes with that property show a reduction of precision order when there are discontinuities caused by the use of flux limiters Boris and Book (1973) van Leer (1974).

Another more sophisticated approach to cure oscillations in compressible flow computation is the essentially non-oscillatory (ENO) family of schemes. These schemes are uniformly accurate and prevent oscillations in the non-smooth regions by detecting discontinuity and modifying the reconstruction stencil from cell to cell and time level to time level. ENO schemes are computationally expensive and sacrifice fast convergence because of their dynamic stencils Wolf (2006) Weighted ENO (WENO) schemes were developed to address the problems caused by dynamic stencils. Near discontinuities, weighted ENO schemes (Abgrall (1994), Gooch (1997), Friedrich (1998)) remove the effect of non-smooth data in

the reconstruction stencil by giving it an asymptotically small weight. However no comprehensive convergence analysis and/or computational cost studies are presented. Furthermore, performance of ENO/WENO schemes in the context of implicit time advance, which is one of the most efficient solution strategies, has not yet been fully explored. The present work also presents some results in this context.

There are in literature many ENO and WENO schemes. Different applications triggers many works, including simulations with interactions between shock waves and turbulence Hu and Shu (1999) Adams and Shariff (1996), simulations of hydrodynamic equations Dolezal and Wong (1995), simulations with interactions between shock waves and vorticity Casper and Atkins (1993) ERLEBACHER *et al.* (1997), simulations of incompressible flows Harten and Chakravarthy (1991), simulations of viscous-elastic flows Shu and Zeng (1997) and even image processing Osher and Sethian (1988). The use of ENO and WENO schemes in non-structured meshes are considered a challenging area Käser and Iske (2005). Wolf Wolf (2006) applied the ENO and WENO schemes in non-structured meshes through a finite volume technique in an existing tool, solving Euler equations in two dimensions.

The Mate Face (MF) is an implicit topological data structure designed to store unstructured meshes. It implements many operators and iterators used to manipulate the mesh. The MF data structure allows the representation of bidimensional meshes (simple 2D or superficial) and three-dimensional meshes (also called volumetric meshes). For a two-dimensional mesh, it can be of simple or hybrid type (triangle and/or quadrilateral), and a volumetric mesh can be only the simple type (which includes tetrahedron, prism, pyramid or hexahedron elements). The MF uses half-edges for superficial meshes and half-faces for volumetric meshes. The representation of vertexes, edges and cells is explicit, while topological operations are implicit.

The MF is a flexible data structure that can represent different mesh types, including meshes with different element types at the same time, such as triangles and quadrilaterals together. It implements a technique of partial allocations of vectors in order to represent vector of elements. In this way, memory blocks are dynamically set, as new elements are added in the mesh. This strategy eases the problem of memory space for vector of elements. The geometric information about the mesh is stored in the vertexes, where each one is associated to position of the space, base for the most of geometric operations. Each vertex in the MF also store a reference to its mate cell through an identification number. The treatment of singularities is also implemented, facilitating diverse query types as star queries and operations on non convex meshes. The edges in MF are represented explicitly, and also stores the adjacent cells that share it. This representation has the advantage that information can be directly stored in the edge, as for example the id of adjacent cells of the edge.

The representation of cells is obtained by storing references to vertexes, edges (and faces in the three-dimensional case). Beyond that, mate cells can be retrieved through incident edges or faces. One consideration about the organization in memory of mesh elements in two-dimensional meshes is that for each cell, the number of vertexes is equal to the number of edges and neighbors. This feature eases the implementation and representation of relationships of neighborhood. Then, by using a counter clock orientation, every neighbor cells are indexed in the mesh.

Besides the available traverse queries, geometric operators are also available, and are very used in the simulation code, such as the distance between two points, the area of a cell, the localization of a given query point (like inside a triangle or on the edge of it), the coordinates of a centroid of a cell, among others. The MF supports loading many mesh file formats, such as VTK and VRML.

In this paper we present a computational study of coupling of a topological data structure, the Mate Face, into a solver module, by controlling all grid access by providing operators and iterators that perform complex neighbor queries. We analyze memory and performance issues about Mate Face mesh indexing applied on a simulation using finite volume technique with a formulation that sets the property values to the control volume centroids, using high order methods - the ENO and WENO schemes. The paper outline is: Section 2 explains the theoretical formulation for equations used to model the physical phenomenon of interest; Section 3 presents the numerical formulation for the simulation; Section 4. presents the reconstruction process for the ENO and WENO high order schemes; Section 5 show the experiments and results for the computational study on mesh indexing approaches and Section 6 draw conclusions about the work.

## 2. THEORETICAL FORMULATION

In this work assumes that the Euler equations correctly represent or model the physical phenomenon of interest. Hence, the viscous and heat transfer terms of the URANS equations are ignored. Moreover, only two-dimensional studies are considered simplifying even further the simulation.

The Euler equations provide significant challenges for numerical methods despite its simplified aspect depicted above. These include non-linear terms and are capable to produce discontinuous solutions even if the initial conditions are smooth. They do provide a great initial start or base to develop, test and verify numerical methods of any sort. The Euler equations in two dimension, written in conservative form can be written as

$$\frac{\partial \mathbf{Q}}{\partial t} + \frac{\partial \mathbf{E}}{\partial x} + \frac{\partial \mathbf{F}}{\partial y} = 0, \quad (1)$$

where

$$\mathbf{Q} = \begin{Bmatrix} \rho \\ \rho u \\ \rho v \end{Bmatrix}, \quad \mathbf{E} = \begin{Bmatrix} \rho u \\ \rho u^2 + p \\ \rho v u \\ (e + p) u \end{Bmatrix}, \quad \mathbf{F} = \begin{Bmatrix} \rho v \\ \rho u v \\ \rho v^2 + p \\ (e + p) v \end{Bmatrix} \quad (2)$$

The final equation system is obtained adding the equation of the pressure  $p$  for a perfect gas.

$$p = (\gamma - 1) \left[ e - \frac{1}{2} \rho |\mathbf{u}|^2 \right]. \quad (3)$$

### 3. NUMERICAL FORMULATION

In the present work, the 2D Euler equations are solved in their integral form as

$$\frac{\partial}{\partial t} \int_V \mathbf{Q} dV + \int_V (\nabla \cdot \mathbf{P}) dV = 0, \quad (4)$$

where  $\mathbf{P} = \mathbf{F}_i + \mathbf{G}_j$ . Applying the Gauss theorem in Equation (4), we have

$$\frac{\partial}{\partial t} \int_V \mathbf{Q} dV + \int_V (\mathbf{P} \cdot \mathbf{n}) dS = 0, \quad (5)$$

where  $V$  represents the volume of the cell,  $S$  represents the surface of the cell and  $\mathbf{n}$  is the unit vector normal to the surface  $S$ . The Equation (5), discretized in a finite volume context centered in cells, can be rewritten for a control volume  $i$  as

$$\frac{\partial \mathbf{Q}_i}{\partial t} = -\frac{1}{V_i} \int_{S_i} (\mathbf{P} \cdot \mathbf{n}) dS, \quad (6)$$

where  $\mathbf{Q}_i$  is the mean value of  $\mathbf{Q}$  at time  $t$ , in the control volume  $V_i$ , defined as

$$\mathbf{Q}_i = \frac{1}{V_i} \int_{V_i} \mathbf{Q} dV. \quad (7)$$

Therefore, a final formulation for a discretization of Euler equations in two dimensions inside a finite volume context is of form

$$\frac{\partial \mathbf{Q}_i}{\partial t} = -\frac{1}{V_i} \sum_{k=1}^{nf} (\mathbf{F}_k \bar{\mathbf{i}} + \mathbf{G}_k \bar{\mathbf{j}}) \cdot \mathbf{S}_k, \quad (8)$$

where  $nf$  is the number of faces, or edges in the two dimensions space, of the volume control.

The control volumes considered in this work are triangles and they can be decomposed into a finite number of line segments  $\Gamma_j$ . One should observe that the control volumes could be composed by any type of polygon, because the really important aspect is that its bounding contour could be decomposed into a finite number of line segments. The surface integral from Equation (5) can be discretized using  $N$ -point Gaussian integration formula

$$\int_{S_i} (\mathbf{P} \cdot \mathbf{n}) dS \approx \sum_j |\Gamma_j| \sum_{l=1}^N w_l \mathbf{P}(\mathbf{Q}_j(\mathbf{G}_1), t) \cdot \mathbf{n}, \quad (9)$$

where  $\mathbf{G}_1$  and  $w_l$  are, respectively, the Gaussian points and the weights on the  $\Gamma_j$  line segment. For the second-order accuracy scheme just one Gauss point is necessary for the integration. Given the coordinates of the points in the corner of the control volume face,  $z_1$  and  $z_2$ , it can be obtained the centroid point of the face,

$$\mathbf{G}_1 = \frac{\mathbf{z}_1 + \mathbf{z}_2}{2}. \quad (10)$$

In the case, the weight,  $w_1$ , is chosen as  $w_1 = 1$ . For the third-order schemes, two Gaussian points are necessary along each line segment. Their values are given by

$$G_1 = \frac{\sqrt{3}+1}{2\sqrt{3}}z_1 + \left(1 - \frac{\sqrt{3}+1}{2\sqrt{3}}\right)z_2 \quad \text{and} \quad G_2 = \frac{\sqrt{3}+1}{2\sqrt{3}}z_2 + \left(1 - \frac{\sqrt{3}+1}{2\sqrt{3}}\right)z_1, \quad (11)$$

where the respective weights,  $w_1$  and  $w_2$  are given by  $w_1 = w_2 = 1/2$

Using the method described above, one can compute values of  $Q_i$  in some instant,  $t$ , and then, from these mean values, one can reconstruct polynomials that represent the primitive variables  $\rho$ ,  $u$ ,  $v$  and  $p$ . Finally, it is possible to compute values of the conserved variables in the Gaussian points. Due to the discontinuity of the reconstructed values of the conserved variables over the cell boundaries, one must use a numerical flux function to approximate these flux values on the cell boundaries. In this paper, we have used the Roe flux difference splitting method Roe (1981) to compute such approximations. An explicit Runge-Kutta scheme of five stages with second order of accuracy was used to obtain the time solution of the governing equations, proposed by Mavriplis (1988).

#### 4. ENO/WENO RECONSTRUCTION

The ENO and WENO schemes were developed for the objective of capturing more efficiently discontinuities that occurs in problems with partial hyperbolic governing equations.

The reconstruction process of ENO schemes basis on the approximation of the mean values of primitive variables for each mesh volume control by polynomials with order lower than the order of wanted spatial precision Wolf (2006). For the building of polynomials of order  $\eta$  it is necessary to use  $N(\eta)$  cells, where  $N(\eta) = (\eta + 1)(\eta + 2)/2$ . For the polynomial reconstruction of each control volume, it is necessary to define a possible set of cells which will compose the stencil molecule. Using a cell centered finite volume discretization, the stencil molecule can be built through the selection of neighbor cells. For a linear reconstruction, which will result in a second order precision scheme, it chooses the primary neighbors of target cell. The primary neighbors are cells that share at least one edge with the target control volume. This process is extended to the case of higher order reconstructions by using secondary neighbors of target control volume. The Mate Face data structure has operators that easy such operations without extra cost.

In the simulation tool, the control volumes can have the triangle or quadrilateral form, then we can evaluate their approximation polynomials as

$$p(x, y) = \sum_{|\beta| \leq \eta} r_{\beta_1 \beta_2} (x - x_c)^{\beta_1} (y - y_c)^{\beta_2} \quad (12)$$

where  $|\beta| = \beta_1 + \beta_2$ , with  $\beta_i \in \{0, 1, 2, \dots\}$ ,  $x_c$  and  $y_c$  are the Cartesian coordinates of volume control's barycenter and  $r_{\beta_1 \beta_2}$  are the polynomial coefficients that represent the approximation for the derivatives of the rebuilt primitive variables. Considering that the integral of  $p(x, y)$  in each stencil molecule returns the mean value of the cell's primitive variable, it is possible to write a linear system,  $[R] = r = \bar{u}$ , composed of  $N(\eta)$  equations with  $N(\eta)$  unknown variables, where the latter are the polynomial coefficients,  $r_{\beta_1 \beta_2}$ . The  $[R]$  represents the matrix of control volume moments, calculated according to Gooch Gooch (1997), by using the scaling technique proposed by Friedrich Friedrich (1998) in order to avoid poorly conditioned matrices. Therefore,  $r$  is the coefficient vector which must be evaluated and  $\bar{u}$  is the vector composed by the mean values in cells for each primitive variable.

The control volume moments that composes the matrix  $[R]$  must be invertible and defined as

$$\overline{x^n y^m}_i \equiv \frac{1}{V_i} \int_{S_i} (x - x_c)^n (y - y_c)^m dS, \quad (13)$$

and are calculated by using a Gauss quadrature formula following the same procedure as the one used in the flux computation.

For each cell, after performing the polynomial reconstruction, the next step is to evaluate which polynomial is the least oscillatory to be used in the ENO scheme. This oscillation is evaluated by using some indicator that assesses the smoothness of  $p(x, y)$ . By the results presented in the literature Friedrich (1998), the oscillation indicator used in the this work is the one proposed by Shu and Jiang (1996). The formulation for oscillation indicator can be written as

$$OI_{JS} [p(x, y)] = \left\{ \sum_{1 \leq |\beta| \leq \eta} \int_{V_i} h^{|\beta|-1} \left[ \frac{\partial^{|\beta|} p(x, y)}{\partial x^{\beta_1} \partial y^{\beta_2}} \right]^2 dx dy \right\}^{\frac{1}{2}} \quad (14)$$

where  $h$  is a mesh width Abgrall (1994).

The WENO schemes use all polynomial rebuild in its formulation, different from ENO schemes. This polynomial are added, multiplied its respective weights, for the construction of a unique approximated polynomial  $p(x, y) = \sum_{k=1}^m \omega_k p_k(x, y)$ . The weights  $\omega_k$  are obtained by oscillation indicators of stencil molecule. They are of order one in the smooth regions of the flow and are of the order of the desired accuracy in the solution in the regions with discontinuities. The weights can be computed as

$$\omega_k = \frac{\epsilon + OI[p_k(x, y)]^{-\theta}}{\sum_{k'=1}^m \{\epsilon + OI[p_{k'}(x, y)]\}^{-\theta}} \tag{15}$$

where  $\epsilon$  has very small magnitude and it is used to avoid zero divisions and  $\theta$  is a positive integer number. The WENO schemes have the property of being very smooth and stable in smooth regions of the flow, but this property is lost if  $\hat{\Delta}$  is chosen too large. In that case the scheme tends to behave like the ENO schemes.

The implementation of reconstruction for the different precision order involve choosing cells in the neighborhood of the target cell to compose the stencil molecule and the polynomial construction. The ideal case is to choose all neighbor cells to compose the stencil molecule, but this is not always the best case. A detailed study about the stencil molecule building process was made by Wolf (2006). Then, the next considerations show the best result of cell choice for the stencil molecule composition by reducing the method oscillations.

In the linear case, the polynomials are built from three cells. The constant term of the polynomial is given by the mean value of the primitive properties of the main volume considered. So, it is necessary to evaluate two coefficients of the linear terms in the interpolation polynomial. This is performed by solving a linear system of two equations.

The better configuration for this reconstruction type is to select a combinations of primary and secondary neighbor cells, in such a way to obtain stability in the method and correction of the oscillations next to the shock waves. An example of a valid configuration for this configuration is shown in Figure 1. In the figure, there are shown two configuration of molecules, one for triangular meshes and another for quadrilateral meshes, where  $V_1$  and  $V_2$  represent the chosen cells to build the stencil molecule.

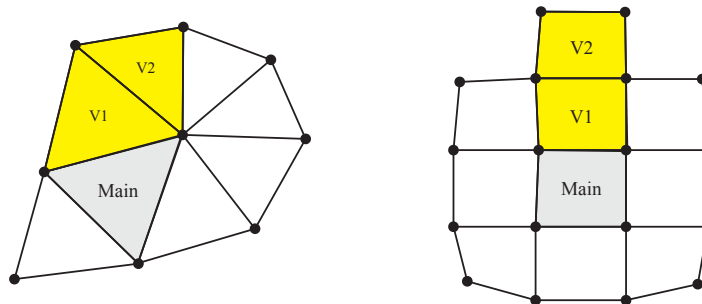


Figure 1. Valid stencil molecule for the reconstruction of second order of precision.

For the reconstruction of second order of precision, the stencil molecule is formed by six cells for the polynomial reconstruction. Again, the constant polynomial coefficient is the mean value of the primitive properties of the main volume. Therefore, it is necessary to obtain two coefficients of linear terms and three coefficients of quadratic terms for the interpolation polynomial, which are obtained by solving a linear system of five equations.

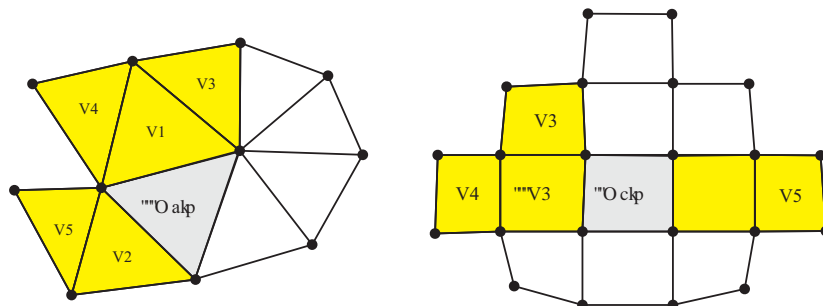


Figure 2. Valid stencil molecule for the reconstruction of third order of precision.

For the reconstruction of fourth order of precision, it is necessary to select ten cells for the polynomial reconstruction. In this case the constant coefficient is also given by the mean value of the primitive properties of the main volume. It is

necessary, then, to obtain two terms of the linear coefficients, three coefficients of the quadratic terms and four coefficients of the cubic terms for the interpolation polynomial, evaluated from a linear system of nine equations.

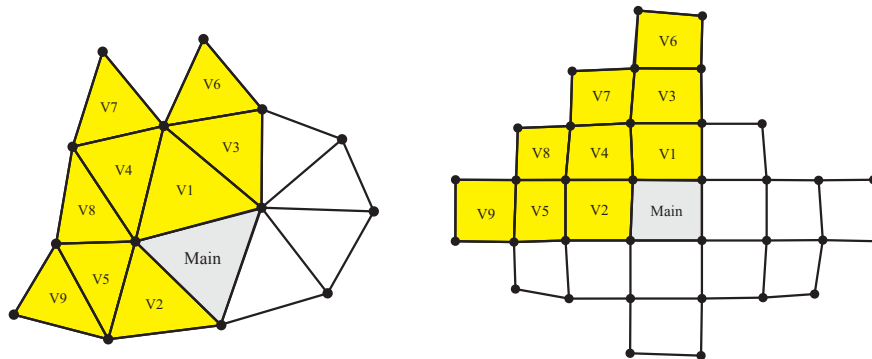


Figure 3. Valid stencil molecule for the reconstruction of fourth order of precision.

## 5. EXPERIMENTS

In this section we first show experiments that include the analysis of the computational cost involved in coupling data structures, in this case the Mate Face, with the detailed solver in Sec. 1. The objective is to show that such data structures are robust to massive data indexing preserving low cost for search operations. Finally, we show experiments validating the usage of the topological data structure with a case test at a NACA 0012 airfoil.

### 5.1 Scalability

This section shows a computational cost analysis of the usage of the Mate Face data structure compared with the internal tables approach at the disk mesh loading step. We measured the time spent and memory occupied when constructing both data structures and the time spent for a complex query operation, the search for elements around a given vertex in the mesh.

For the experiments, it was used four meshes NACA 0012 with different number of elements (refinements). They are described in the table 1. Note that the number of vertexes and cells increase for each mesh file.

Mesh	Number of vertexes	Number of Cells
1	5908	11634
2	6995	13744
3	7363	14400
4	9100	17844

Table 1. Different NACA 0012 mesh files used in the experiments.

The cost analysis was performed by measuring the time spent for building the data structures and also the amount of memory allocated for each of them. In order to accomplish this task over different mesh sizes, it was performed a scalability test using all meshes. Therefore, the statistics were obtained by indexing in both data structures over different mesh sizes.

Figure 4 shows the time spent for building which consists of reading the mesh from system file, allocating memory for indexing data and assigning data to the data structure. For the numbered mesh files, a higher number of elements will demand more processing time. From the figure, it can be seen that the building cost for Mate Face is much lower than the internal tables approach. The Mate Face presents a linear behavior and can index up to 10 times faster than the internal tables approach.

Another measure we present is the comparison of allocated main memory for each approach. Although in the Mate Face all neighbor elements are obtained in constant time, it represents cells, edges and faces explicitly, i.e., allocating memory for that information. But a faster indexing data structure it is important for applications that deals with large mesh files or multiple of them.

Figure 5 shows comparatively the memory cost bound to every approach, varying the number of elements in each

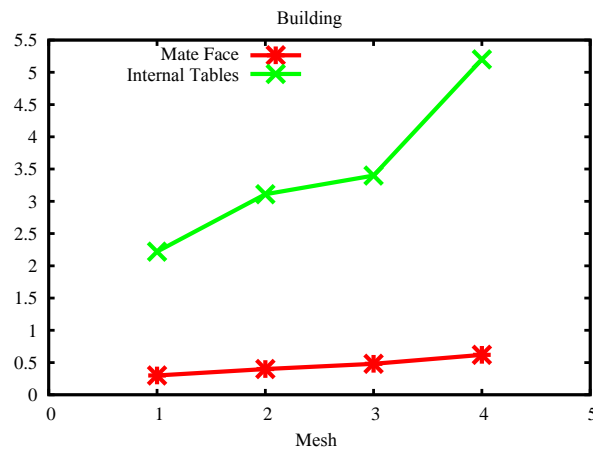


Figure 4. Building time spent for the different approaches.

mesh to obtain a stability measure. From the figure, it can be seen that besides the Mate Face allocates more memory for small meshes than the internal tables, they approximates as the number of elements increase in the mesh.

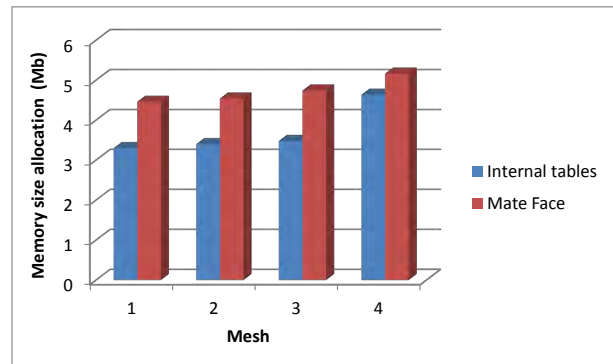


Figure 5. Memory allocation for Mate Face and internal tables approaches.

Figure 6 shows memory growing rate for both approaches, using the same mesh files. The label (1,2) indicates the growing rate between mesh 1 and 2, and so on. The results are presented in logarithmic scale representing the growing rate in percent. From Fig. 6, it can be seen that the memory growing rate for Mate Face is lower than the internal tables approach, which implies that the Mate Face is scalable in memory consumption.

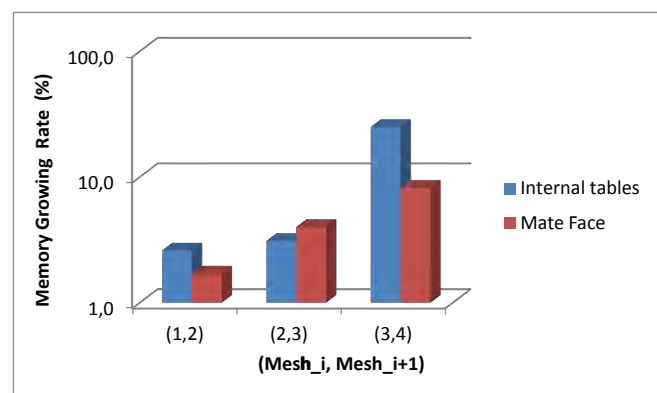


Figure 6. Memory growing rate for Mate Face and internal tables approaches.

After the data structures are built, most of the query operations performed by the Mate Face have constant complexity due to its explicitly representation of the vertexes, cells and edges. But for complex operations like star query (a query which retrieves all neighbors from a given vertex) is not explicit and demand processing time to execute.

An experiment measuring the total time spent to execute 50 times a star query for all vertexes was performed for both approaches, the Mate Face and the internal tables. The internal tables approach precomputes all queries during building

step, so the answer of a given query relies on accessing a matrix field. In this experiment we compute the total time spent for Mate Face to perform fifty times the star query for the whole dataset. Table 2 shows the obtained results, and it can be seen that the Mate Face executes all queries in less than one second. We conclude that the Mate Face performance for queries is acceptable based on this result.

Mesh	Internal tables	Mate Face
1	0.01	0.54
2	0.01	0.64
3	0.01	0.67
4	0.01	0.85

Table 2. Total time spent for star queries (seconds).

The computational costs analyzed reinforces the concept that a specialized data structure for mesh manipulation is adequate and have advantages when indexing large number of elements for numeric simulations. Results showed that Mate Face is faster to build, presents a better growing rate for memory allocation and perform complex queries at a suitable performance.

## 5.2 NACA 0012

This test case considers the transonic flow over a NACA 0012 airfoil with one degree of incidence. Two cases were tested, using two mesh files with different number of vertexes and elements (triangles). The Mach number of free stream was considered as  $M_\infty = 1.0$ . Figure 7 shows the schema representation of the flow in this case.

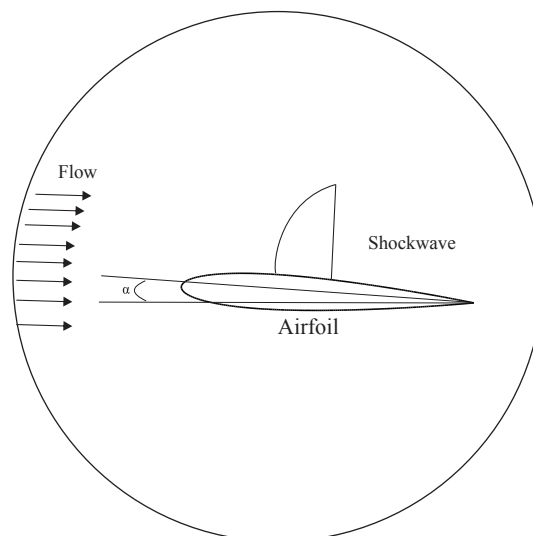


Figure 7. Scheme representation of airfoil NACA 0012 flow.

The WENO schema with reconstruction order 4 of precision was used in experiments, with Jiang and Shu indicator, Roe method for numeric flow evaluation on edges, and a three stage TVD Runge Kutta for time march. The density was made dimensionless with respect to density of free flow and the pressure was made dimensionless with respect to the density times squared sound speed.

Figure 8 shows obtained results from the simulation of the density at computational domain, in both implementations. From the graphs, it can be seen that the results are very similar, reinforcing that the same mesh and input parameters was used for the two tests. The shown results were generated by using the Tecplot 360<sup>1</sup> visualization tool.

Another result achieved is shown in Fig. 9, which is related to the distribution of pressure coefficient ( $C_p$ ) on the upper camber of the airfoil, showing results for both approaches. The smoothness indicators of Jiang and Shu were used in the simulators.

<sup>1</sup><http://www.tecplot.com>

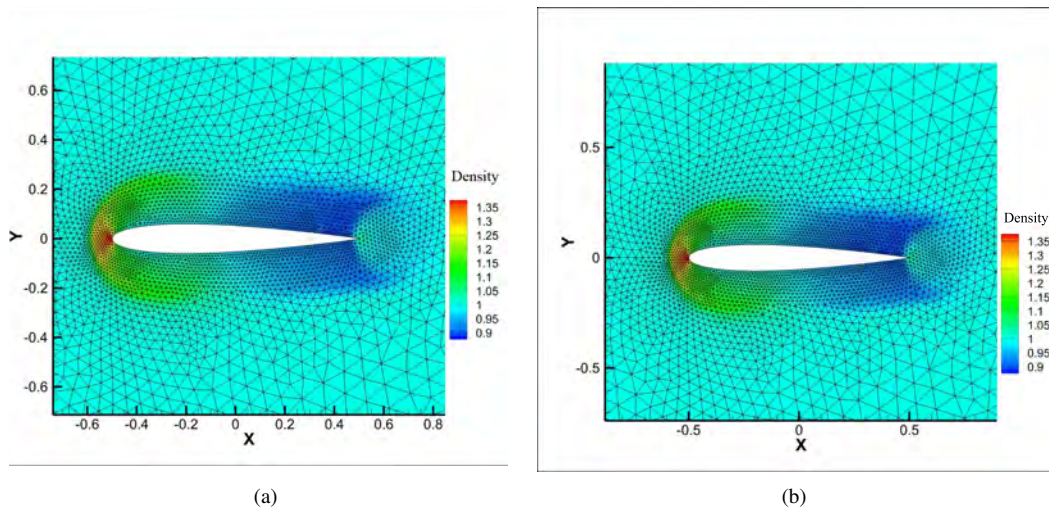


Figure 8. Density results. (a) Density of domain by simulator with the internal tables approach. (b) Density of domain by the simulator with the Mate Face structure.

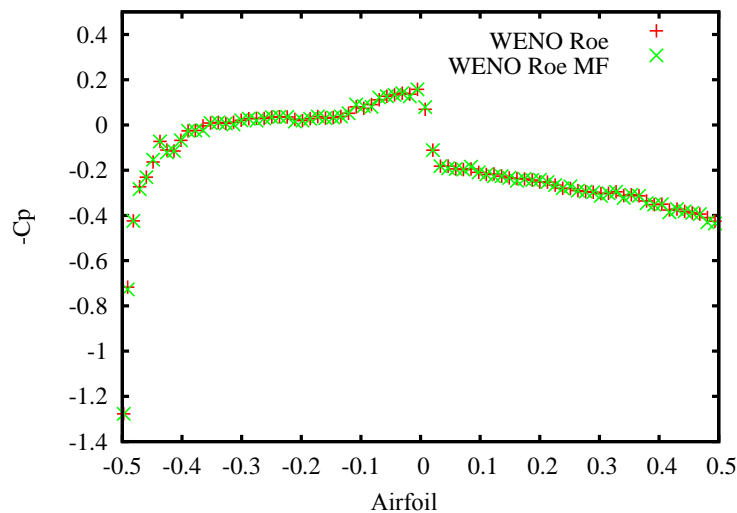


Figure 9. Distribution of the pressure coefficient on the upper camber of the airfoil, with  $M_1 = 1.0$  and  $\alpha = 1.0$ .

## 6. CONCLUSION

In this paper we presented a computational study of coupling of a topological data structure, the Mate Face, into a solver module, that controls all grid access by providing operators and iterators that perform complex neighbor queries. In experiments, we presented occupied memory and performance results about Mate Face mesh indexing against the traditional representation of matrices for the mesh. We study case was a simulation using finite volume technique with a formulation that sets the property values to the control volume centroids, using high order methods - the ENO and WENO schemes. The results showed that Mate Face is faster to build than the traditional approach, and presents a better growing rate for memory allocation for large mesh files and also perform complex queries at a suitable performance.

## 7. ACKNOWLEDGEMENTS

The authors acknowledge the support provided to the present research by Fundação de Amparo à Pesquisa do Estado de São Paulo, FAPESP, under Grant No. 2008/01544-6.

F. Barbosa, I. Pola, A. Castelo  
Performance Analysis of Data Structures for Unstructured Grid Solutions On Finite Volume Simulations.

## 8. REFERENCES

- Abgrall, R., 1994. "On essentially non-oscillatory schemes on unstructured meshes: Analysis and implementation". *Journal of Computational Physics*, Vol. 114, No.1, pp. 45–58.
- Adams, N. and Shariff, K., 1996. "A high-resolution hybrid compact-eno scheme for shock-turbulence interaction problems". *Journal of Computational Physics*, Vol. 127, No. 1, pp. 27 – 51. ISSN 0021-9991. doi:10.1006/jcph.1996.0156.
- Anderson, W., 1963. "A comparison of finite volume flux vector splittings for the euler equations". *American Institute of Aeronautics and Astronautics - AIAA*. doi:doi:10.2514/6.1985-122.
- Azevedo, J.A.L.F., Figueira da Silva, L.A.s.F. and Strauss, D., 2010. "Order of accuracy study of unstructured grid finite volume upwind schemes". *Journal of the Brazilian Society of Mechanical Sciences and Engineering*, Vol. 32, pp. 78 – 93. ISSN 1678-5878.
- Boris, J.P. and Book, D.L., 1973. "Flux corrected transport: I. shasta, a fluid transport algorithm that works". *Journal of Computational Physics*, Vol. 11, No. 1, pp. 38–69.
- Casper, J. and Atkins, H.L., 1993. "A finite-volume high-order eno scheme for two-dimensional hyperbolic systems". *J. Comput. Phys.*, Vol. 106, No. 1, pp. 62–76. ISSN 0021-9991. doi:10.1006/jcph.1993.1091. URL <http://dx.doi.org/10.1006/jcph.1993.1091>.
- Dolezal, A. and Wong, S., 1995. "Relativistic hydrodynamics and essentially non-oscillatory shock capturing schemes". *Journal of Computational Physics*, Vol. 120, No. 2, pp. 266 – 277. ISSN 0021-9991. doi:10.1006/jcph.1995.1164. URL <http://www.sciencedirect.com/science/article/pii/S0021999185711643>.
- ERLEBACHER, G., HUSSAINI, M.Y. and SHU, C.W., 1997. "Interaction of a shock with a longitudinal vortex". *Journal of Fluid Mechanics*, Vol. 337, pp. 129–153. doi:10.1017/S0022112096004880. URL <http://dx.doi.org/10.1017/S0022112096004880>.
- Friedrich, O., 1998. "Weighted essentially non-oscillatory schemes for the interpolation of mean values on unstructured grids". *Journal of Computational Physics*, Vol. 144, N. 1, pp. 194–212.
- Gooch, C.F.O., 1997. "High order eno schemes for unstructured meshes based on least-squares reconstruction". Technical Report P631-1296, Argonne National Laboratory, Mathematics and Computer Science Division.
- Harten, A. and Chakravarthy, S.R., 1991. *Multi-Dimensional ENO Schemes for General Geometries*. Tech. Rep. 91–76, ICASE.
- Hu, C. and Shu, C.W., 1999. "Weighted essentially non-oscillatory schemes on triangular meshes". *Journal of Computational Physics*, Vol. 150, No. 1, pp. 97 – 127. ISSN 0021-9991. doi:10.1006/jcph.1998.6165. URL <http://www.sciencedirect.com/science/article/pii/S0021999198961654>.
- Käser, M. and Iske, A., 2005. "Ader schemes on adaptive triangular meshes for scalar conservation laws". *J. Comput. Phys.*, Vol. 205, No. 2, pp. 486–508. ISSN 0021-9991. doi:10.1016/j.jcp.2004.11.015. URL <http://dx.doi.org/10.1016/j.jcp.2004.11.015>.
- Liou, M.S., 1996. "A sequel to ausm+". *Journal of Computational Physics*, Vol. 129, No. 2, pp. 364–382.
- Mavriplis, D.J., 1988. "Multigrid solution of the two-dimensional Euler equations on unstructured triangular meshes". *AIAA Journal*, Vol. 26, No. 7, pp. 824–831.
- Osher, S. and Sethian, J.A., 1988. "Fronts propagating with curvature-dependent speed: algorithms based on hamilton-jacobi formulations". *J. Comput. Phys.*, Vol. 79, No. 1, pp. 1–49.
- Roe, P.L., 1981. "Approximate riemann solver, parameter vectors". *Journal of Computational Physics*, Vol. 43, pp. 357–372.
- Shu, C.W. and Jiang, G., 1996. "Efficient implementation of weighted eno schemes". *Journal of Computational Physics*, Vol. 126, pp. 202–228.
- Shu, C.W. and Zeng, Y., 1997. "High-order essentially non-oscillatory scheme for viscoelasticity with fading memory". *Q. Appl. Math.*, Vol. LV, No. 3, pp. 459–484. ISSN 0033-569X. URL <http://dl.acm.org/citation.cfm?id=262735.262741>.
- van Leer, B., 1974. "Towards the ultimate conservative difference scheme. ii. monotonicity and conservation combined in a second order scheme". *Journal of Computational Physics*, Vol. 14, No. 4, pp. 361–370.
- Van Leer, B., 1982. "Flux-vector splitting for the euler equations". *Lecture Notes in Physics*, Vol. 170, pp. 507–512.
- Wolf, W.R., 2006. *Simulação de Escoamentos Aerodinâmicos Compressíveis Utilizando Esquemas Não Oscilatórios de Alta Ordem de Precisão em Malhas Não Estruturadas*. Ph.D. thesis, Instituto Tecnológico de Aeronáutica, São José dos Campos-SP.